Received: 13 April 2017 | Accepted: 20 July 2017
DOI: 10.1002/jcp.26109

ORIGINAL RESEARCH ARTICLE

WILEY Journal of Cellular Physiology

Electric fields accelerate cell polarization and bypass myosin action in motility initiation

Yao-Hui Sun[1,2] | Yuxin Sun[1] | Kan Zhu[1,3] | Brian Reid[1] | Xing Gao[1] | Bruce W. Draper[4] | Min Zhao[1] | Alex Mogilner[2]

[1] Department of Dermatology and Department of Ophthalmology, University of California, Davis School of Medicine, Sacramento, California

[2] Courant Institute and Department of Biology, New York University, New York, New York

[3] Bioelectromagnetics Laboratory, Zhejiang University, School of Medicine, Hangzhou, Zhejiang, China

[4] Department of Molecular and Cellular Biology, University of California Davis, One Shields Avenue, Davis, California

Correspondence
Min Zhao, Department of Dermatology and Department of Ophthalmology, University of California, Davis School of Medicine, Sacramento 95817, CA.
Email: minzhao@ucdavis.edu
Alex Mogilner, Department of Molecular and Cellular Biology, University of California Davis, One Shields Avenue, Davis 95616, CA.
Email: mogilner@cims.nyu.edu

Funding information
Air Force Office of Scientific Research, Grant number: FA9550-16-1-0052; Center for Scientific Review, Grant numbers: EY019101, GM068952

Stationary symmetrical fish keratocyte cells break symmetry and become motile spontaneously but slowly. We found that applying electric field (EF) accelerates the polarization by an order of magnitude. While spontaneously polarized cells move persistently for hours, the EF-induced polarity is lost in a majority of cells when the EF is switched off. However, if the EF is applied for a long time and then switched off, the majority of cell move stably. Myosin inhibition abolishes spontaneous polarization, but does not slow down EF-induced polarization, and after the EF is turned off, motility does not stop; however, the cell movements are erratic. Our results suggest that the EF rapidly polarizes the cells, but that resulting polarization becomes stable slowly, and that the EF bypasses the requirement for myosin action in motility initiation.

KEYWORDS
cell polarization, galvanotaxis, motility initiation, myosin

1 | INTRODUCTION

Three distinct aspects of cell migration—cell polarization, cell motility, and directional sensing—are complex on their own, and each can arise without the other two (Iglesias & Devreotes, 2008) yet in physiological phenomena they are interconnected. Many cell types can polarize spontaneously: *Dictyostelium* cells spontaneously break symmetry, acquire distinct leading and rear edges, and migrate randomly (Li, Norrelykke, & Cox, 2008). Fibroblasts self-polarize in stages regulated by multiple molecular checkpoints that control the contractile-adhesive system (Prager-Khoutorsky et al., 2011). Epithelial cells spontaneously switch to a migratory polarized phenotype after relaxation of their actomyosin cytoskeleton as a result of competition between protrusive and contractile actin networks around the cell edge (Lomakin et al., 2015). Cells also polarize in response to chemotactic gradients and then move directionally up these gradients (Iglesias & Devreotes, 2008), in a manner that is cell-specific.

Present Address of Yuxin Sun, Department of Radiology and Biomedical Imaging, University of California San Francisco, 505 Parnassus Ave, M-372, Box 0628, San Francisco 94143–0628, CA.

One of the model systems used to unravel the complex crosstalk between polarization, motility, and directional sensing is fish epithelial keratocytes. Stationary symmetric keratocyte cells undergo spontaneous polarization (SP) and become motile within tens of minutes; the motility initiates from the prospective rear (Barnhart, Lee, Allen, Theriot, & Mogilner, 2015; Yam et al., 2007). During SP, adhesion strength drops across the whole cell, but more so at the prospective rear, as a result of an adhesion stick-slip switch (Barnhart et al., 2015); this leads to accelerated centripetal flow at the rear that retracts the rear and allows the front to protrude. As the cell starts to move, myosin is swept to the rear; its contraction retracts the cell rear, contains the cell sides, and together with actin polymerization at the front keeps the cell moving. An additional mechanical module—a treadmill of polarized actin network inside the plasma membrane—can maintain the steady motility (Barnhart, Lee, Keren, Mogilner, & Theriot, 2011; Ofer, Mogilner, & Keren, 2011) but is unable to polarize the stationary cell (Barnhart et al., 2015; Yam et al., 2007).

One of the ubiquitous directional signals is an endogenous electric field (EF) in the order of 1 V/cm that occurs naturally during development (Altizer et al., 2001), cancer (Pu et al., 2007; Wu, Ma, & Lin, 2013) and wound healing, (Zhao et al., 2006) and polarize cells and guide their migration. Many types of cells, from bacteria and yeast (Minc & Chang, 2010) to mammalian cells, from Dictyostelium to keratinocytes, from nerve cells to fibroblasts, polarize and migrate directionally in an EF (Patel & Poo, 1982; Huang, Samorajski, Kreimer, & Searson, 2013; Yang, Charles, Hummler, Baines, & Isseroff, 2013; Zhao, Jin, McCaig, Forrester, & Devreotes, 2002). Keratocytes sense the EF and move to the cathode (Allen, Mogilner, & Theriot, 2013; Cooper & Schliwa, 1986).

Electric effects are as important in polarization as in directional sensing (Chang & Minc, 2014). One particular striking example is membrane depolarization and polarity switch upon contact between two types of pigment cells in zebrafish skin, melanophore, and xanthophore, causing melanophore to migrate away from the xanthophore, which is the basis of skin stripe emergence (Inaba, Yamanaka, & Kondo, 2012). Studies of yeast and plant cells have started to uncover molecular mechanisms of polarization that involve ion channels, transmembrane electric potential, and intracellular pH (reviewed in [Chang & Minc, 2014]). There was little investigation of the polarizing effect of EF in motility initiation of animal cells (Chang & Minc, 2014; Wu et al., 2013). A recent insightful study (Saltukoglu et al., 2015) addressed these effects in motility initiation of human keratinocytes and found that low extracellular pH reverses the direction of polarization. Other than the directional effect of the EF, there was no significant difference in the process of cell polarization with and without EF, perhaps because keratinocytes are slow. This implies that the internal polarization mechanism that is completely downstream of EF sensing is the time-limiting factor in the dynamics of symmetry breaking for these cells. It was also discovered that zebrafish keratocytes lose polarity in the absence of extracellular Ca^{2+}, but regain polarity in an EF (Graham, Huang, Robinson, & Messerli, 2013).

There are many open questions about EF-induced polarization (EFP) versus SP, among them: does the EF accelerate polarization? Are mechanochemical pathways of EFP the same as those of SP? Is myosin contractility necessary for the EFP? To answer these questions, we used quantitative measurements of dynamic cell shapes during spontaneous and EF-induced polarization of fish keratocyte cells combined with pharmacological inhibition. We find that the EF accelerates the polarization by an order of magnitude and bypasses requirement for myosin in motility initiation. Interestingly, while spontaneously initiated motility is stable, the polarization induced by a short-term EF application is unstable. However, a long-term EF application stabilizes cell motility.

2 | MATERIALS AND METHODS

2.1 | Keratocyte isolation and primary culture

The Institutional Animal Use and Care Committees of the University of California at Davis approved the animal procedures used in this study (protocol number 16478), which were performed in accordance with NIH guidelines. Scales of Central American cichlid *Hypsophrys nicaraguensis* were removed from the flanks and allowed to adhere to the bottom of a culture dish (Barnhart et al., 2011; Sun et al., 2016). The scales were covered by a 22-mm glass coverslip with a stainless steel nut on the top to hold it in position, and cultured at room temperature in Leibovitz's L-15 media (Gibco BRL, Gaithersburg, MD), supplemented with 14.2 mm HEPES pH 7.4, 10% Fetal Bovine Serum (Invitrogen, Carlsbad, CA), and 1% antibiotic-antimycotic (Gibco BRL). Sheets of keratocytes that migrate off the scale after 24–48 h were dissociated by a brief treatment with 0.25% Trypsin/0.02 EDTA solution (Invitrogen) in phosphate buffered saline (PBS). Isolated keratocytes were kept on ice until use.

2.2 | Pharmacological treatments

Cells were seeded in EF chambers and incubated at room temperature for up to 30 min to allow attachment. For perturbation experiments, drugs (all purchased from Sigma–Aldrich, St. Louis, MO) were added to the culture medium at the following concentrations: DMSO (0.1%), LY294002 (50 or 150 μm), Blebbistatin (50 μm), and CK-666 (50 μm). Subsequent experiments were implemented in the presence of a drug within 15 min of incubation.

2.3 | EF application and time-lapse recording

The EF was applied as previously described (Song et al., 2007; Zhao, Agius-Fernandez, Forrester, & McCaig, 1996) in custom-made electrotaxis chambers (20 mm × 10 mm × 0.1 mm). The chambers were built over tissue culture-treated dishes. These custom-made electrotaxis chambers with small cross-sectional area provide high resistance to current flow and minimize Joule heating during EF application. To eliminate toxic products from the electrodes that might be harmful to cells, agar salt bridges made with 1% agar gel in Steinberg's salt solution were used to connect silver/silver chloride electrodes in beakers of Steinberg's salt solution to pools of excess

medium at either side of the chamber. EF strength is empirically chosen based on our previous studies (Sun et al., 2013). In most experiments an EF of 4 V/cm was used unless otherwise indicated. The actual voltage is measured by a voltmeter before and after each experiment. Phase contrast images were captured by a Zeiss Observer Z1 microscope (Carl Zeiss, Thornwood, NY) equipped with a Quan-tEM:512SC EMCCD camera (Photometrics, Tucson, AZ). Time-lapse experiments were performed using MetaMorph NX software controlling a motorized scanning stage (Carl Zeiss) at room temperature. Typically, in each experiment four fields at magnification of 20× were captured sequentially. Images were taken at 10 or 30 sec interval except the high resolution ones for the demonstration purpose, which were taken at 1 sec interval under a 40x objective. Time-lapse images were imported into ImageJ (http://rsbweb.nih.gov/ij). Tracks were marked by using the MtrackJ tool and plotted by using the Chemotaxis tool as described (Sun et al., 2013).

2.4 | Defining morphological characterization and polarization

Phase contrast images of keratocytes were converted into binary images using custom-written Matlab codes. Briefly, we used Matlab edge detection and a basic morphology function to outline cells in the phase contrast image. We used the Otsu method (Otsu, 1979) to erase the halo artifacts. If shape was still unsatisfactory, we then used the Lasso tool in Photoshop (Adobe) to manually draw the cell shape. Polygonal outlines extracted from the binary images were plotted in Celltool, an open source software (Pincus & Theriot, 2007). Geometric features of each cell, including centroid, area and aspect ratio, were measured directly from the polygons using standard formulas (Barnhart et al., 2011). The aspect ratio was calculated as the ratio of the width to the length of a cell and was used to determine if a cell was polarized or un-polarized. To define polarization, we conducted a pilot experiment and traced a large number of cells undergoing SP. The significant polarization was detected around 15 min. We then calculated the standard deviation of the aspect ratio at this time point (214 cells were analyzed). A value out of range of mean ± SD (0.8547–1.1687) is treated as polarized (Supplemental Figure S1).

2.5 | Aligning contours and mapping edge velocity

Serial polygonal outlines of a cell were extracted from time-lapse images and sampled at 200 evenly spaced points. These contours were then mutually and sequentially aligned to simulate cell motion over time (Pincus & Theriot, 2007). For the first frame of a time-lapse sequence, the contour was adjusted manually to make sure that the first point "0" locates right in the middle facing cathode (Supplemental Figure S2c). The cell boundary positions were translated to polar coordinates. The edge velocity at each point was calculated by dividing the displacement vector normal to the cell edge by the time interval (Barnhart et al., 2011). A custom scalar map function written in Matlab was used to generate continuous space-time plots of protrusion and retraction. For visualization efficiency, all maps are plotted in three colors.

2.6 | Shape principal component analysis

Similar to the alignment procedure described above, polygons extracted from a large population of cells after different drug treatments with no EF stimulation were mutually aligned together. Principal models of shape variation were determined by principal component analysis of the population of polygonal cell outlines, and scaled in terms of the standard deviation of the population for each mode of variation, which was detailed previously (Barnhart et al., 2011).

2.7 | Statistics

In most cases a representative experiment is shown; additional images and data are shown in the Supplementary Figures. Data are presented as means ± standard deviation. To compare group differences either chi-squared test or paired/unpaired, two-tailed Student's *t*-test was used. A *p*-value less than 0.05 is considered as significant.

3 | RESULTS

3.1 | EF accelerates motility initiation to cathode

We used time-lapse phase contrast microscopy and measurements of cell shapes and spatial-temporal distributions of protrusion/retraction velocity around the dynamic cell edge (edge velocity maps) (see, Materials and Methods and Supplemental Figure S1) to compare SP and EFP. In agreement with (Barnhart et al., 2015; Yam et al., 2007), without EF cells remained symmetrical, disc-like, and their center-of-mass did not translocate for tens of minutes (Figure 1a). The majority of cells did not undergo SP within 30 min (Figure 1e; Supplemental Figure S1d). In the unpolarized state, cells were not static: most of them exhibited waves of protrusion-retraction around the edge easily identifiable by the diagonal patterns on the edge velocity maps (Figure 1b; Supplemental Figure S2a). Such waves, observed at the leading edge of polarized keratocytes moving on highly adhesive surfaces (Barnhart et al., 2011), indicate that the protrusive dynamics are excitable when membrane tension is high (Allard & Mogilner, 2013).

We observed that a physiological-strength EF accelerated polarization by an order of magnitude, from tens of minutes to a few minutes (Figures 1a, 1b, and 1e; Supplemental Figures S2a and S2b; Table S1; Video S1). Half of the cells were polarized within 6 min, and after 20 min almost all cells became motile (Figure 1e; Supplemental Table S1). The cells polarized not in a random direction, but to the cathode, and continued to move to the cathode persistently (Figure 1a; Supplemental Figure S2; Table S1; Video S1). Protrusion and retraction were biased to the cathode and anode, respectively, in seconds after the EF was turned on (Figure 1b). Almost always, there were no protrusion-retraction waves around the edge prior to EFP (Figure 1b; Supplemental Figure S2b).

To confirm that cells exhibit a directional response, and not only react to the amplitude of an EF, and to estimate the time to initiate motility, we applied EF periodically, switching its polarity every 2 min.

We observed that the stationary cells do not initiate motility in the alternating EF (Supplemental Video S2). As a rule, local protrusions and retractions appeared at the cathodal and anodal sides, respectively, switching places around the cell in synchrony with the EF, but the characteristic morphology of the motile cell did not have time to evolve. When, after periodic directionality switching, EF polarity stops changing, the cell initiates steady motility to the cathode (Supplemental Video S2). Thus, while the EF signal is transduced in seconds to tens of seconds, the cytoskeletal machinery needs minutes for global reorganization.

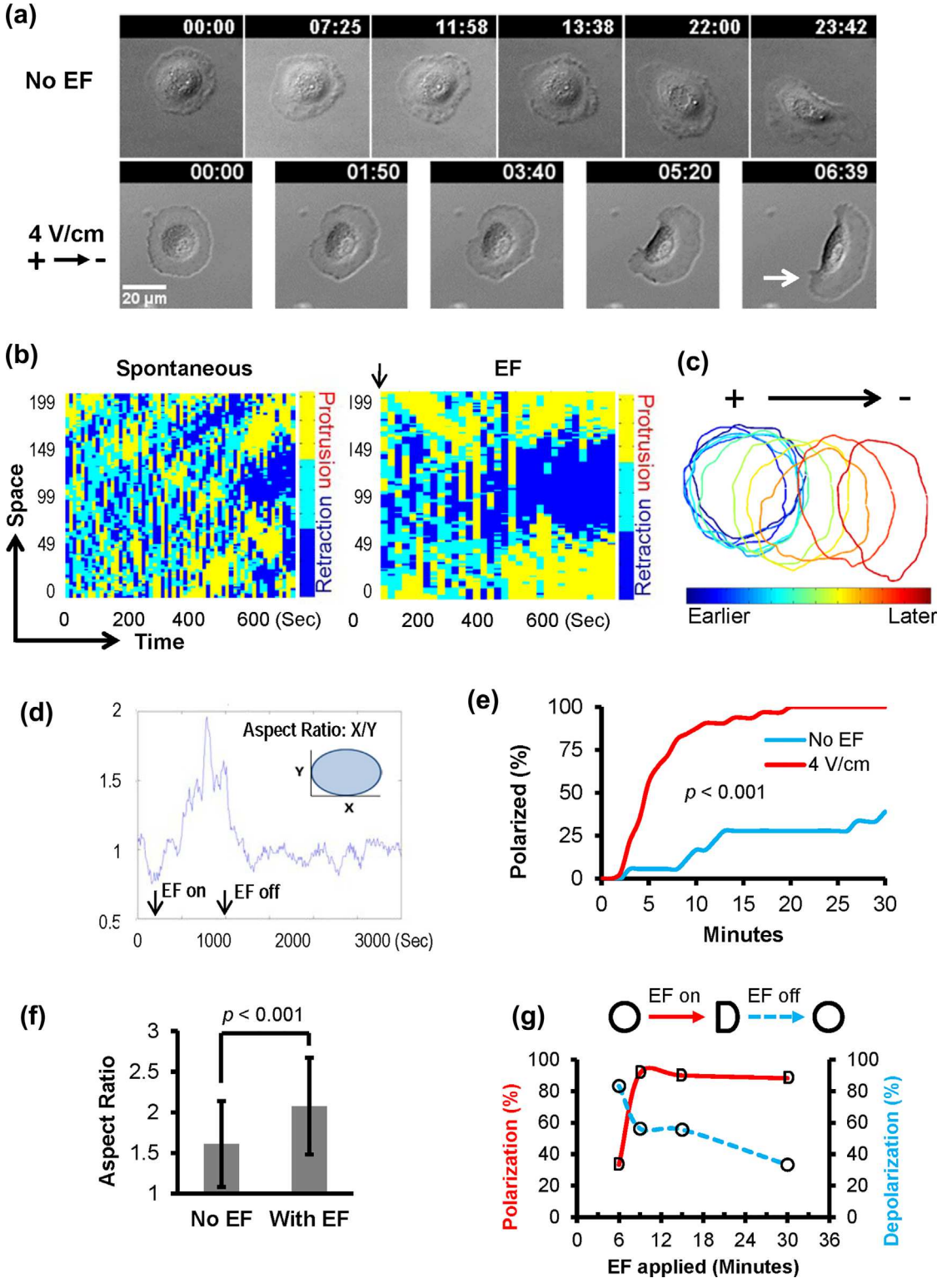

FIGURE 1 Continued.

3.2 | EFP induced by short-term EF application is unstable, but EFP induced by long-term EF application is stable

We noticed that although the EF accelerates the motility initiation, a significant fraction of cells depolarize and stop when the EF is switched off (Figures 1d and 1g, Supplemental Table S2). Meanwhile, cells that were already polarized and motile before the EF was switched on keep moving to cathode in the EF, and then remain polarized and keep moving in a random direction when the EF is switched off (Supplemental Table S2). This suggests that the EF induces polarization into a state different from that evolving in SP. However, as the duration of the time interval when the EF is on increases, the fraction of cells losing polarity decreases (Figure 1g, Supplemental Table S2, Figure S2d): more than four out of five cells depolarized when the EF was applied for only 6 min, while only half of the cells depolarized when the EF was applied for 10–15 min, and two-thirds of the cells continued to move after the EF was switched off after being on for 30 min (Figure 1g). This suggests that the unstable EF-induced motile state matures into the stable one within tens of minutes providing the EF is on during the maturation.

3.3 | Cells polarize from the rear both in SP and EFP

It is known that keratocytes polarize spontaneously from the prospective rear (Barnhart et al., 2015; Yam et al., 2007), where accelerated centripetal actin flow creates a local cell boundary retraction. We confirmed these observations (Figure 1a; Supplemental Video S1; Figure S2a): the initiation of motility could be best identified by development of the flat rear edge from the original round edge retracting to the cell body, while the rounded opposite edge became the leading edge without significant shape change. We then observed that in the EF, the symmetry break started, similarly, by caving in of the prospective rear (Figures 1a and 1c; Supplemental Figures S3b and S3c; Video S1).

3.4 | Cells polarize rapidly and bidirectionally when PI3 is inhibited

PI3 kinase-mediated signaling is required for polarization in a number of cell types (Iglesias & Devreotes, 2008), but no effect of PI3 K inhibitor LY294002 compound at a concentration of 50 μm on keratocyte polarization was previously detected (Yam et al., 2007). We confirmed this result (Supplemental Table S1): in the EF, when LY294002 concentration was 50 μm, the cells polarized rapidly to the cathode. However, when LY294002 concentration was increased to 150 μm, the cells polarized rapidly, but half of the cells − to cathode, and half − to anode (Supplemental Table S1). This is in agreement with the observation in (Sun et al., 2013) that, when PI3 K is inhibited in already motile cells, some start migrating to cathode, others—to anode, with a slight majority crawling to anode. This effect was interpreted in (Sun et al., 2013) as a tug-of-war between two signaling pathways, one of which, PI3K-independent is normally weaker and tries to orient the cell to anode, and another, strong and PI3K-dependent, orienting the cell to cathode. Our results here indicate that the same two pathways likely to operate not only in orienting polarized cells, but also during the emergence of the cell polarity and motility initiation.

3.5 | EF can induce polarization without myosin contractility

Myosin-driven contractility in keratocytes, on the other hand, is crucial for SP in general and initial retraction of the prospective cell rear in particular (Barnhart et al., 2015; Yam et al., 2007). We confirmed that myosin inhibition by Blebbistatin largely stops SP (Figure 2d). A natural hypothesis would be that the EF simply orients the protrusion-contraction axis of the cell and that inhibition of myosin impairs the polarization in the EF, too.

Surprisingly, we found that Blebbistatin-treated cells polarized rapidly, within 10–15 min, to the cathode (Figures 2a and 2d; Supplemental Figure S3; Table S1; Video S3). The polarization initiated at the prospective rear at the anodal side (Figure 1b; Supplemental

FIGURE 1 EFs accelerate polarization. (a) Time-lapse images show spontaneous polarization and EF-initiated polarization (4 V/cm in the indicated orientation). Subsequently this cell underwent directional migration to the cathode (white arrow). Time is in mm:ss. Scale bar is 20 μm. (b) Edge velocity maps of spontaneous and EF-induced polarization. Yellow represents protrusion of the cell boundary, and dark blue represents retraction. Spontaneous polarization proceeds through transient protrusion/retraction waves. In the EF (applied at time 0, arrow), protrusion/retraction is focused from the start. The spatial coordinates around the cell edge are calibrated as shown in Supplemental Figure S2c. (c) Sequential cell contours during 30 min of EF application. (d) Aspect ratio of a representative cell with the EF on and off as shown. Aspect ratio is defined as the X/Y ratio where X is the width and Y is the length of a cell, as shown in the inset (more precisely, X and Y are the width and length of the cell's bounding rectangular box). A value out of range of the mean control aspect ratio ± SD (0.8547–1.1687), that was pre-calculated from cells during 15 min of no-treatment ($n = 214$), was defined as polarized. (e) Dynamic change of the percentage of polarized cells plotted for keratocytes exposed to no EF (blue line; $n = 24$) or EF of 4 V/cm (red line; $n = 22$). A significant difference was determined by an unpaired two-sample Student's t-test ($p < 0.001$). (F) Aspect ratio of cells 45 min after no EF ($n = 94$) or EF of 4 V/cm ($n = 80$) exposure. Data is presented as mean ± SD from a representative of repeated experiments. A significant difference was determined by an unpaired two-sample Student's t-test ($p < 0.001$). (g) Polarization rates induced by an EF of 4 V/cm (red arrow at the top) applied for 6, 9, 15, and 30 min respectively, and depolarization rates at 15 minutes after EF was switched off (blue arrow at the top). Polarization and depolarization were quantified from measuring the aspect ratios of $n = 29$, 45, 21, and 29 keratocytes for each time point, respectively. (See, EF-independent polarization rates in Supplementary Table S2)

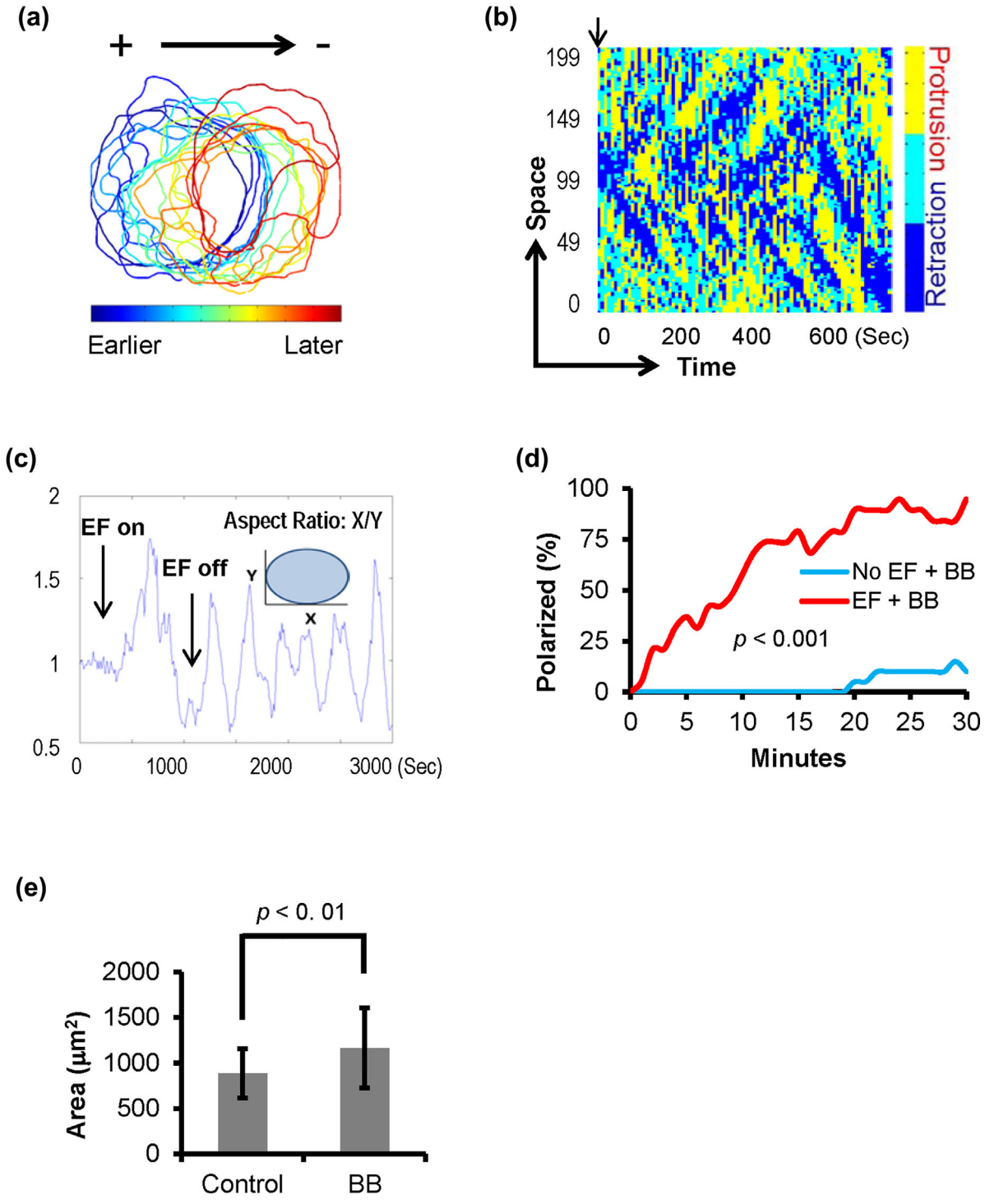

FIGURE 2 EFP in the presence of myosin inhibitor (Blebbistatin). (a) Sequential cell contours during 30 min of an EF application (4 V/cm in the indicated orientation). (b) Edge velocity map; the color scheme and time scale are the same as in Figure 1b. The arrow indicates when an EF was applied. Note the strong protrusive and retractive waves initiating at the anodal side and propagating towards the cathodal side. (c) Example of dynamics of cell aspect ratio with EF on and off. (d) Dynamic change of the percentage of polarized cells is plotted for keratocytes exposed to no EF (blue line; $n = 20$) or EF of 4 V/cm (red line; $n = 19$). A significant difference was determined by an unpaired two-sample Student's t-test ($p < 0.001$). (e) Areas of un-polarized cells after a 30 min exposure of mock control ($n = 42$, mean = 885 μm^2, SD = 271 μm^2) and 50 μM myosin inhibitor ($n = 32$, mean = 1166 μm^2, SD = 439 μm^2). A significant difference was determined by an unpaired two-sample Student's t-test ($p < 0.001$)

Figure S3; Table S1; Video S3). The motility pattern consisted of periodic cycles of protrusion-retraction waves propagating at the sides of the cell from the rear to the front (Figure 2b, Supplemental Figure S3b).

Similar to spontaneously polarized cells and in contrast to cells that underwent EFP, motile cells did not stop and depolarize when the EF was switched off (Figure 2c, Supplemental Video S3), but continued to move, however unsteadily (Figures 2a and 2c, Supplemental Video S3). This suggests that the EF bypasses the requirement of myosin for polarization, but unlike motility with functional myosin and without the EF, the EF-induced myosin-inhibited motility is more erratic: cell shape oscillates, aspect ratio fluctuates periodically, and trajectory meanders (Figures 2a and 2c, Supplemental Figure S3a, Video S3).

We observed that the cell area is increased when myosin is inhibited (Figure 2e), which likely indicates an elevated membrane tension (Lieber, Yehudai-Resheff, Barnhart, Theriot, & Keren, 2013). Thus, we hypothesize that the focusing of the protrusion to the front and resulting higher membrane tension could assist the polarization. To test this hypothesis, we used CK–666 to partially inhibit Arp2/3, and therefore protrusion, in the presence of the EF. We found that only 50% of the Arp2/3-inhibited cells were polarized, compared to almost all control cells being polarized in the EF by that time (Supplemental Table S1).

4 | DISCUSSION

Fish keratocyte cells can break symmetry and initiate motility spontaneously in tens of minutes. One of the most visible effects of EFs on these fast-moving cells is that an EF accelerates polarization by an order of magnitude: the EF signal is transduced to the cytoskeleton in seconds, and the cytoskeletal machinery needs only minutes for global reorganization into the motile state. EFP starts from the prospective rear, similar to SP. We found that the nature of polarization in an EF is different from spontaneous motility initiation: the latter is usually unconditionally stable, and the polarized cell moves in a random direction for hours. If the EF is turned on while the cell is already moving, the cell goes to the cathode, and when EF is off, the cell keeps moving randomly. In contrast, after EFP the cell moves to the cathode, but only as long as the EF is on; when the EF is turned off, the majority of cells depolarize and stops if the EF was applied for less than about 20 min. However, if the EF is applied for a longer time the fraction of cells that continue to move after the EF is off grows, and the majority of EF-induced motile cells exhibit stable movement without the EF if the EF is kept on for 30 min.

The critical limiting step of SP in keratocytes is switching of adhesions from the strong "stick" state to the weak "slip" state at the prospective cell rear, which takes tens of minutes (Barnhart et al., 2015; Yam et al., 2007). We hypothesize that EF rapidly focuses protrusion to the cathodal side of the cell, generates the membrane tension and induces motility bypassing the adhesion switch into the slip mode at the rear. If the EF is switched off before the adhesion stick-slip switch takes place, the cell stops after the EF is off. However, if the EF is on for at least about 20 min, the adhesion stick-slip switch occurs, and the cell becomes unconditionally motile. Future studies will be needed to test this hypothesis. A physiological implication of our findings is that the EF tightly controls the short-term motility and directionality of cells in wounds and developmental processes allowing them to polarize and move only when the EF is on. A similar argument was made in (Cohen, James Nelson, & Maharbiz, 2014).

Myosin contraction is critical for SP, yet we found that an EF bypasses this requirement for myosin in polarization. However, myosin-driven contraction is needed to stabilize the cell movement; without myosin the rear remains wobbly. Interestingly, without functional myosin, the cells do not stop when the EF is off.

What could be the mechanism of the EF-induced myosin-inhibited motility initiation? High membrane tension could overcome adhesions and actin network resistance at the rear in the presence of the persistent protrusion at the front, as suggested by (Ofer et al., 2011). We hypothesize that the EF focuses actin protrusion to the cathodal side, generating membrane tension sufficient to crush the actin network at the opposite, anodal side, creating initial local edge retraction.

Use of CK–666 to partially inhibit Arp2/3 in the presence of the EF supports this hypothesis. The percentage of the Arp2/3-inhibited cell polarizing in the presence of EF is still higher than that of the control cells in the EF, so it is possible that the EF, in addition to having an effect on the protrusion at the front, exerts an effect at the anodal side of the cell by relaxing the cell-substrate adhesion there. Interestingly, half of the Arp2/3-inhibited cells polarized to cathode, and half—to anode. Comparison with similar result from PI3 K inhibition indicates that cytoskeletal and signaling pathways are intertwined in a complex, yet to be elucidated, way in galvanotaxis.

The myosin-inhibited cells polarize rapidly in EF, so the reason they do not lose polarity when the EF is turned off early on is not because they have enough time to stabilize the global cytoskeleton reorganization during the onset of migration. We hypothesize that when myosin is inhibited, there are no strong, mature adhesions at the cell periphery induced by myosin-generated pulling. Therefore, when the EF is switched off soon after the motility initiation in the myosin-inhibited cells, there are no strong adhesions at the rear to stop the retraction at the anodal side. The protrusion at the front is not stalled and keeps utilizing the membrane tension to retract the rear in the absence of the rear adhesion.

There are strong similarities between chemotactic and galvanotactic pathways. In fact, while some signaling pathways are specific for galvanotaxis, others are shared with chemotaxis (Gao et al., 2015), and so it is no wonder then that there are similarities between polarization in EF and in a chemical gradient. For example, a strong chemotactic stimulus can also directly elicit de novo production of a pseudopod (Swanson & Taylor, 1982). In chemotaxis, due to adaptation, some types of cells that are polarized in a gradient stop when the stimulus is removed (reviewed in [Jilkine & Edelstein-Keshet, 2011]). Future studies will be required to identify crucial molecular transducers and crosstalks between signaling and cytoskeletal mechanical pathways in galvanotaxis.

ACKNOWLEDGMENTS

This work was supported by National Institutes of Health grant No. GM068952 and by Army Office of Research grant No. 70744-MA to A.M., by National Institutes of Health grant No. EY019101 to M.Z. and by Air Force Office of Scientific Research grant No. AFOSR/RTB FA9550-16-1-0052 to M.Z.

ORCID

Alex Mogilner http://orcid.org/0000-0001-5302-2404

REFERENCES

Allard, J., & Mogilner, A. (2013). Traveling waves in actin dynamics and cell motility. *Current Opinion in Cell Biology*, *25*, 107–115.

Allen, G. M., Mogilner, A., & Theriot, J. A. (2013). Electrophoresis of cellular membrane components creates the directional cue guiding keratocyte galvanotaxis. *Current Biology*, *23*, 560–568.

Altizer, A. M., Moriarty, L. J., Bell, S. M., Schreiner, C. M., Scott, W. J., & Borgens, R. B. (2001). Endogenous electric current is associated with normal development of the vertebrate limb. *Developmental Dynamics*, *221*, 391–401.

Barnhart, E. L., Lee, K. C., Keren, K., Mogilner, A., & Theriot, J. A. (2011). An adhesion-dependent switch between mechanisms that determine motile cell shape. *PLoS Biology*, *9*, e1001059.

Barnhart, E., Lee, K. C., Allen, G. M., Theriot, J. A., & Mogilner, A. (2015). Balance between cell-substrate adhesion and myosin contraction determines the frequency of motility initiation in fish keratocytes. *Proceedings of the National Academy of Sciences of the United States of America*, *112*, 5045–5050.

Chang, F., & Minc, N. (2014). Electrochemical control of cell and tissue polarity. *Annual Review of Cell and Developmental Biology*, *30*, 317–336.

Cohen, D. J., James Nelson, W., & Maharbiz, M. M. (2014). Galvanotactic control of collective cell migration in epithelial monolayers. *Nature Materials*, *13*, 409–417.

Cooper, M. S., & Schliwa, M. (1986). Motility of cultured fish epidermal cells in the presence and absence of direct current electric fields. *The Journal of Cell Biology*, *102*, 1384–1399.

Gao, R. C., Zhao, S. W., Jiang, X. P., et al. (2015). A large-scale screen reveals genes that mediate electrotaxis in Dictyostelium discoideum. *Science Signaling*, *8*, ra50.

Graham, D. M., Huang, L., Robinson, K. R., & Messerli, M. A. (2013). Epidermal keratinocyte polarity and motility require Ca(2)(+) influx through TRPV1. *Journal of Cell Science*, *126*, 4602–4613.

Huang, Y. J., Samorajski, J., Kreimer, R., & Searson, P. C. (2013). The influence of electric field and confinement on cell motility. *PUBLIC LIBRARY OF SCIENCE*, *8*, e59447.

Iglesias, P. A., & Devreotes, P. N. (2008). Navigating through models of chemotaxis. *Current Opinion in Cell Biology*, *20*, 35–40.

Inaba, M., Yamanaka, H., & Kondo, S. (2012). Pigment pattern formation by contact-dependent depolarization. *Science*, *335*, 677.

Jilkine, A., & Edelstein-Keshet, L. (2011). A comparison of mathematical models for polarization of single eukaryotic cells in response to guided cues. *PLoS Computational Biology*, *7*, e1001121.

Li, L., Norrelykke, S. F., & Cox, E. C. (2008). Persistent cell motion in the absence of external signals: A search strategy for eukaryotic cells. *PUBLIC LIBRARY OF SCIENCE*, *3*, e2093.

Lieber, A. D., Yehudai-Resheff, S., Barnhart, E. L., Theriot, J. A., & Keren, K. (2013). Membrane tension in rapidly moving cells is determined by cytoskeletal forces. *Current Biology*, *23*, 1409–1417.

Lomakin, A. J., Lee, K. C., Han, S. J., Bui, D. A., Davidson, M., Mogilner, A., & Danuser, G. (2015). Competition for actin between two distinct F-actin networks defines a bistable switch for cell polarization. *Nature Cell Biology*, *17*, 1435–1445.

Minc, N., & Chang, F. (2010). Electrical control of cell polarization in the fission yeast Schizosaccharomyces pombe. *Current Biology*, *20*, 710–716.

Ofer, N., Mogilner, A., & Keren, K. (2011). Actin disassembly clock determines shape and speed of lamellipodial fragments. *Proceedings of the National Academy of Sciences of the United States of America*, *108*, 20394–20399.

Otsu, N. (1979). A threshold selection method from gray-level histograms. *IEEE Transactions on Systems, Man and Cybernetics*, *9*, 62–66.

Patel, N., & Poo, M. M. (1982). Orientation of neurite growth by extracellular electric fields. *The Journal of Neuroscience: The Official Journal of The Society for Neuroscience*, *2*, 483–496.

Pincus, Z., & Theriot, J. A. (2007). Comparison of quantitative methods for cell-shape analysis. *Journal of Microscopy*, *227*, 140–156.

Prager-Khoutorsky, M., Lichtenstein, A., Krishnan, R., Rajendran, K., Mayo, A., Kam, Z., & Bershadsky, A. D. (2011). Fibroblast polarization is a matrix-rigidity-dependent process controlled by focal adhesion mechanosensing. *Nature Cell Biology*, *13*, 1457–1465.

Pu, J., McCaig, C. D., Cao, L., Zhao, Z., Segall, J. E., & Zhao, M. (2007). EGF receptor signalling is essential for electric-field-directed migration of breast cancer cells. *Journal of Cell Science*, *120*, 3395–3403.

Saltukoglu, D., Grunewald, J., Strohmeyer, N., Bensch, R., Ulbrich, M. H., Ronneberger, O., & Simons, M. (2015). Spontaneous and electric field-controlled front-rear polarization of human keratinocytes. *Molecular Biology of the Cell*, *26*, 4373–4386.

Song, B., Gu, Y., Pu, J., Reid, B., Zhao, Z., & Zhao, M. (2007). Application of direct current electric fields to cells and tissues in vitro and modulation of wound electric field in vivo. *Nature Protocols*, *2*, 1479–1489.

Sun, Y., Do, H., Gao, J., Zhao, R., Zhao, M., & Mogilner, A. (2013). Keratocyte fragments and cells utilize competing pathways to move in opposite directions in an electric field. *Current Biology*, *23*, 569–574.

Sun, Y. H., Sun, Y., Zhu, K., Draper, B. W., Zeng, Q., Mogilner, A., & Zhao, M. (2016). An experimental model for simultaneous study of migration of cell fragments, single cells, and cell sheets. *Methods in Molecular Biology*, *1407*, 251–272.

Swanson, J. A., & Taylor, D. L. (1982). Local and spatially coordinated movements in Dictyostelium discoideum amoebae during chemotaxis. *Cell*, *28*, 225–232.

Wu, D., Ma, X., & Lin, F. (2013). DC electric fields direct breast cancer cell migration, induce EGFR polarization, and increase the intracellular level of calcium ions. *Cell Biochemistry and Biophysics*, *67*, 1115–1125.

Yam, P. T., Wilson, C. A., Ji, L., Hebert, B., Barnhart, E. L., & Theriot, J. A. (2007). Actin-myosin network reorganization breaks symmetry at the cell rear to spontaneously initiate polarized cell motility. *The Journal of Cell Biology*, *178*, 1207–1221.

Yang, H. Y., Charles, R. P., Hummler, E., Baines, D. L., & Isseroff, R. R. (2013). The epithelial sodium channel mediates the directionality of galvanotaxis in human keratinocytes. *Journal of Cell Science*, *126*, 1942–1951.

Zhao, M., Agius-Fernandez, A., Forrester, J. V., & McCaig, C. D. (1996). Directed migration of corneal epithelial sheets in physiological electric fields. *Investigative Ophthalmology and Visual Science*, *37*, 2548–2558.

Zhao, M., Jin, T., McCaig, C. D., Forrester, J. V., & Devreotes, P. N. (2002). Genetic analysis of the role of G protein-coupled receptor signaling in electrotaxis. *The Journal of Cell Biology*, *157*, 921–927.

Zhao, M., Song, B., Pu, J., et al. (2006). Electrical signals control wound healing through phosphatidylinositol-3-OH kinase-gamma and PTEN. *Nature*, *442*, 457–460.

SUPPORTING INFORMATION

Additional Supporting Information may be found online in the supporting information tab for this article.

How to cite this article: Sun Y-H, Sun Y, Zhu K, et al. Electric fields accelerate cell polarization and bypass myosin action in motility initiation. *J Cell Physiol*. 2018;233:2378–2385. https://doi.org/10.1002/jcp.26109

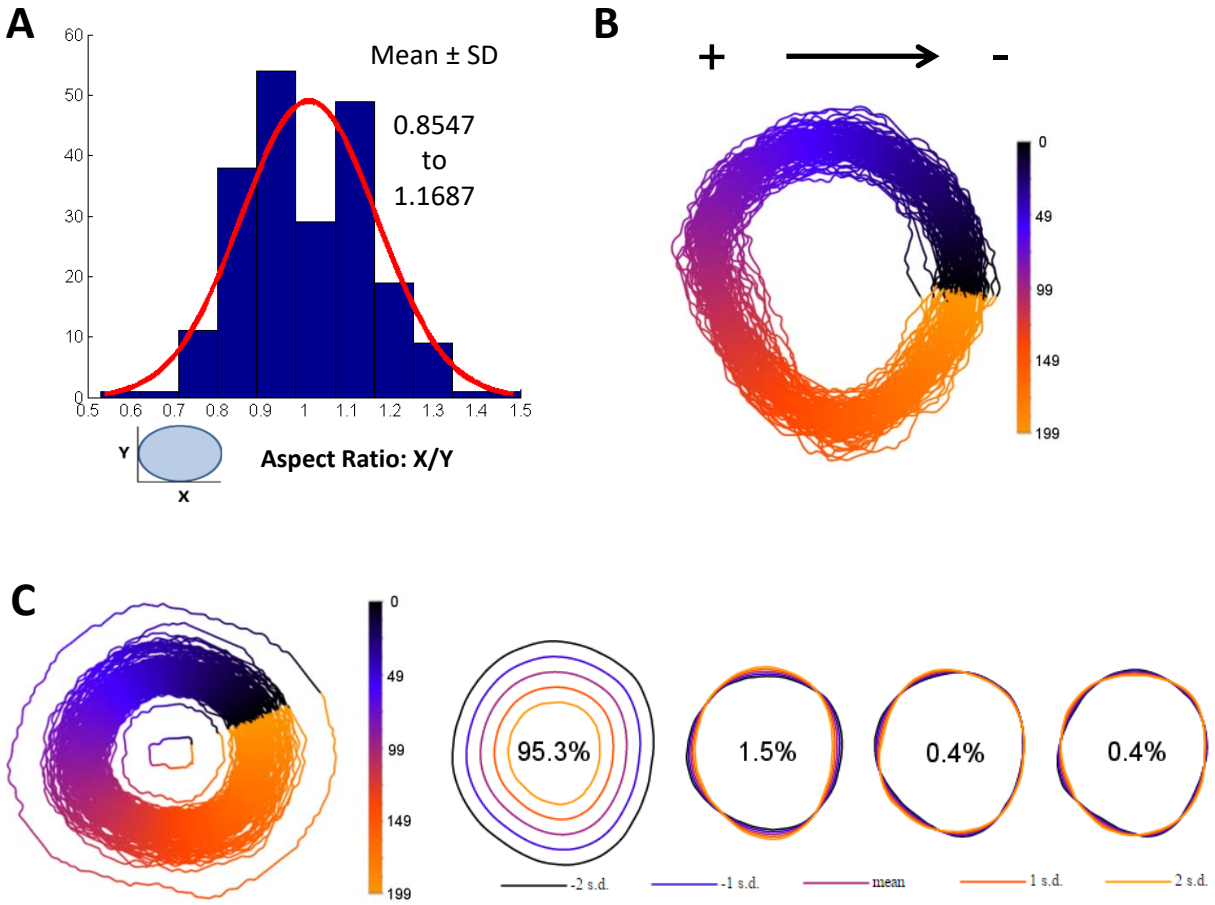

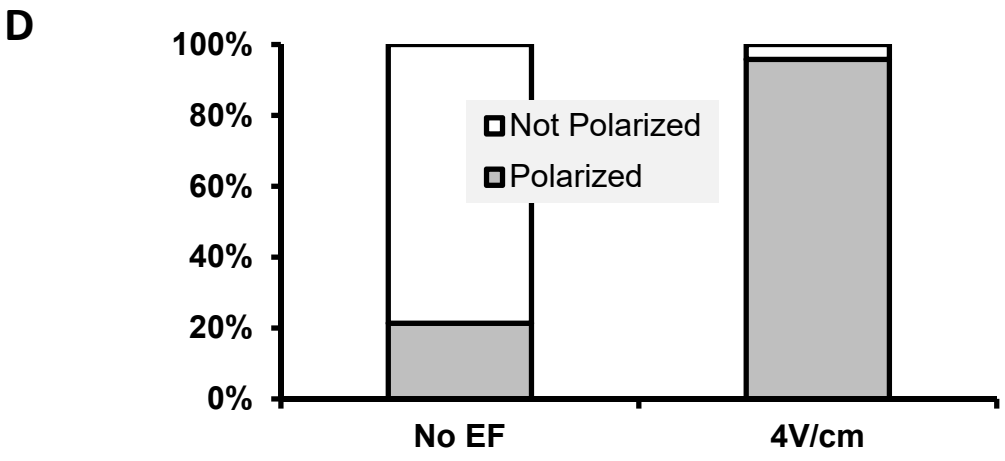

Cells counted	178	119
Not Polarized (%)	78.65	4.20
Polarized (%)	21.35	95.80

SFigure 1

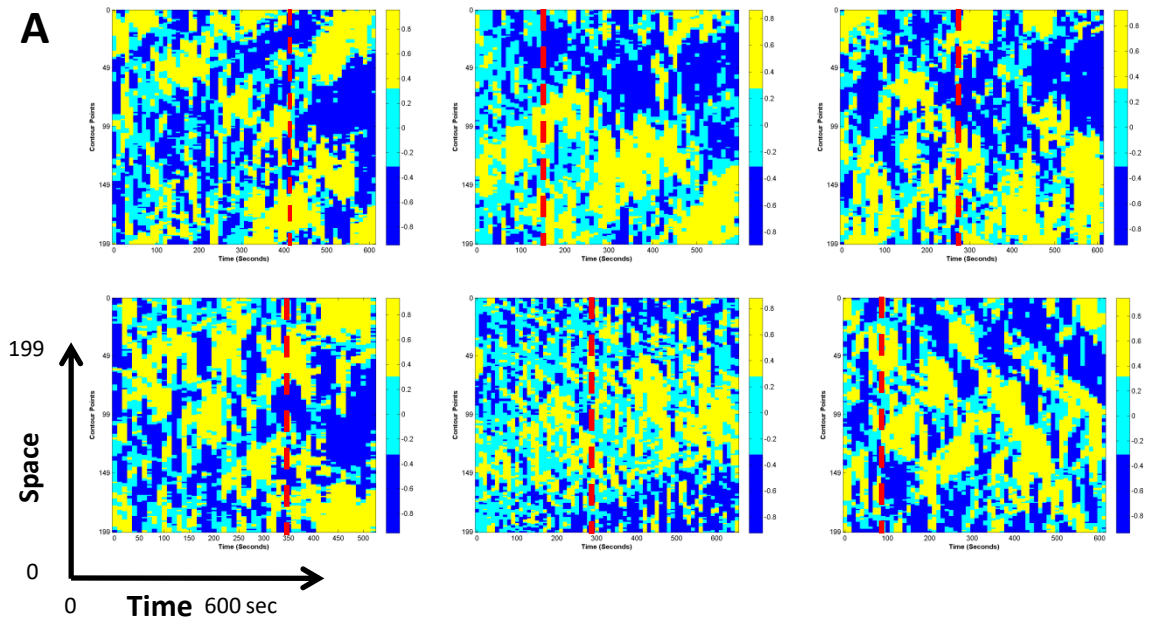
A
199
Space
0
0
Time 600 sec

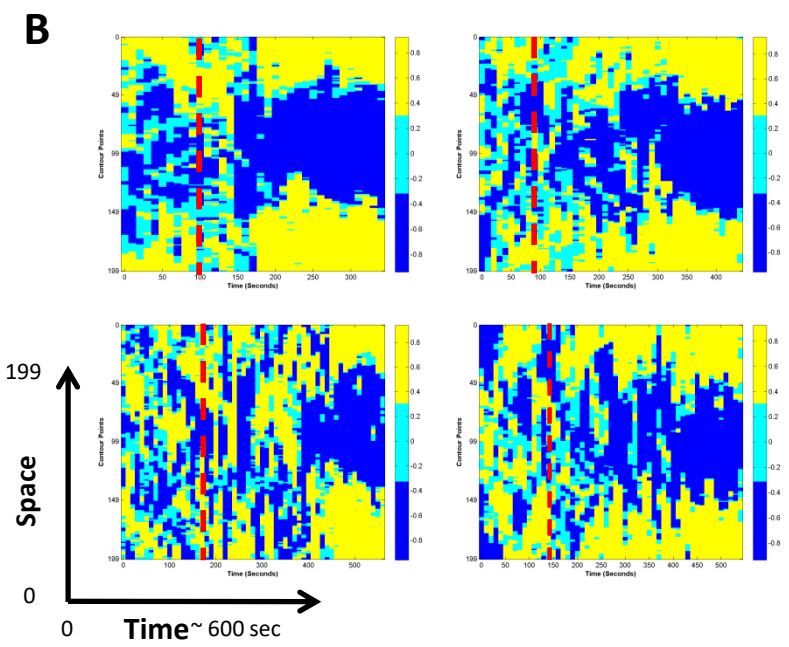
B
199
Space
0
0
Time~ 600 sec

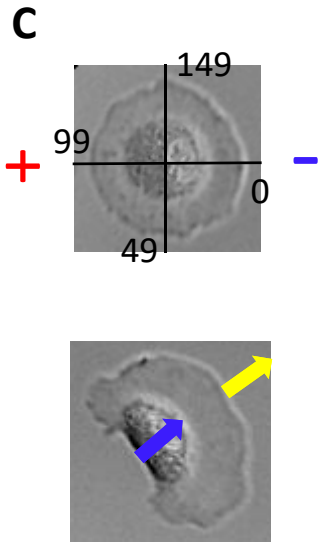
C
149
99
0
49
+
-

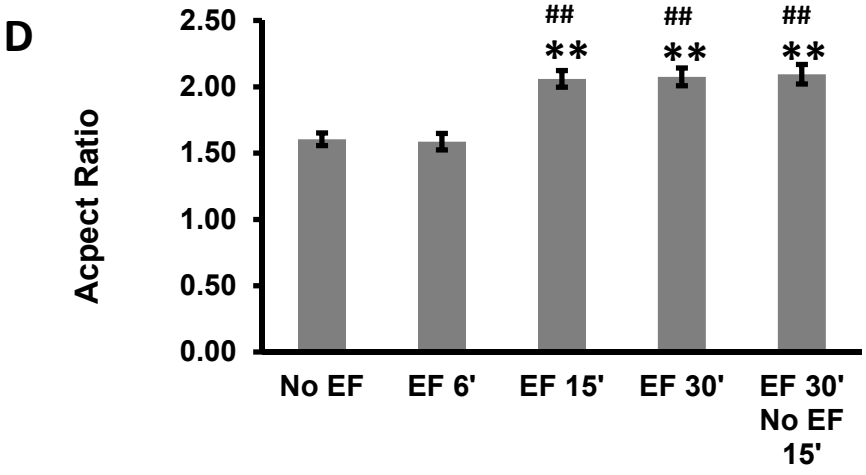
D
Acpect Ratio
2.50
2.00
1.50
1.00
0.50
0.00
##
**
No EF
EF 6'
EF 15'
EF 30'
EF 30' No EF 15'

SFigure 2

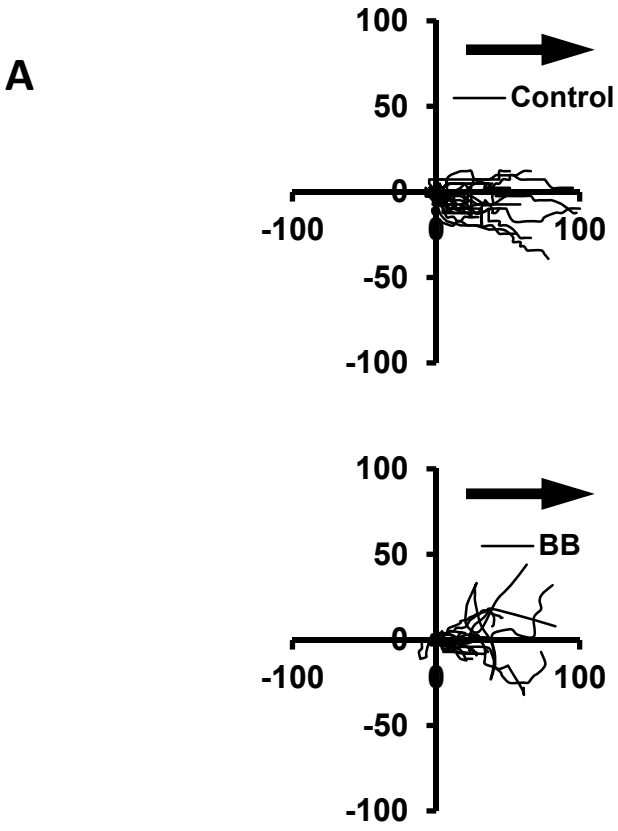

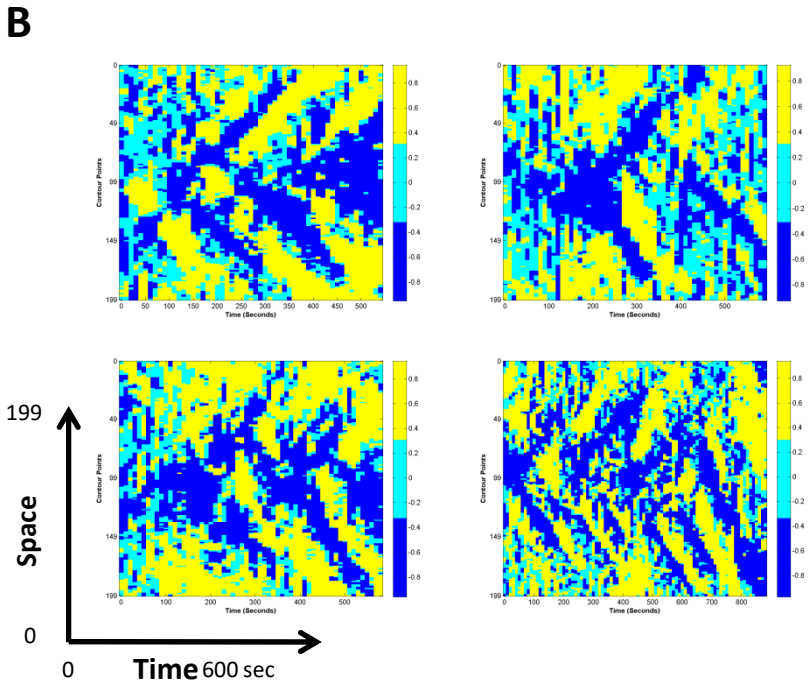

SFigure 3

Supplemental Table 1: Summary of EF-induced polarization

Drugs	Un-polarized (%) [a]	Anode (%) [b]	Cathode (%) [c]
Control	12.08	0.00	87.92
LY 50 µM	4.00	4.00	92.00
BB	5.26	0.00	95.74

[a] Data is presented as percentage of the total polarized cells after EF (4 V/cm) application for 30 minutes
[b] Polarized to anode
[c] Polarized to cathode

Supplemental Table 2: EF-induced polarization is lost after EF is off

EF application [a]	EF-induced polarization (%) [b]	EF-dependent Depolarization (%) [c]	EF-independent polarization (%) [d]
6 minutes	33.33	83.33	100.00
9 minutes	91.43	56.25	100.00
15 minutes	90.00	55.56	81.82
30 minutes	88.24	33.33 *	100.00

[a] EF of 4 V/cm was applied for the indicated time, then switched off and cells were monitored for another 30 minutes
[b] Calculated as (EF-induced polarized cells)/(non-polarized cells before EF application)
[c] Calculated as (Depolarized cells after EF off)/(EF-induced polarized cells)
[d] Calculated as (Still polarized or motile cells after EF off)/(Polarized or motile cells before EF application)
* Difference is significant compared to “6 minutes” by chi-squared test ($p < 0.05$)

Supplemental Figures and Videos

Supplemental Figure 1: Analysis of cell shape in polarization.

A. Distribution of aspect ratios. In a pilot experiment, statistically significant polarization was observed after 15 minutes of time-lapse recording. We pooled all cells within these 15 minutes (n > 1000) and calculated the mean and standard deviation of aspect ratio of each cell. Aspect ratio is defined as X/Y where X is the width and Y is the length of the cell (more precisely, X and Y are the width and length of the cell's bounding rectangular box). A value out of range of mean control ± SD (0.8547 to 1.1687) is defined as polarized.

B. Sampling cell boundary and aligning contours. Cell outlines were extracted from binary images in ImageJ using a custom-written script. 200 points of each cell outline were sampled and consecutive contours aligned using Celltool software (see Materials and Methods for details). Arrow indicates EF orientation.

C. Combined principal modes of shape variation, as determined by principal component analysis of aligned cell outlines, show roundness of the un-polarized cells (n > 200). For each mode, the mean cell shape and shapes one and two standard deviations from the mean are shown. The variation accounted for by each mode is indicated.

D. Rates of SP and EFP after the EF exposure. Data is presented as percentages of polarized and un-polarized cells after 30 minutes with (n = 119) or without (n = 178) the EF (4 V/cm).

Supplemental Figure 2: Additional edge velocity maps of SP and EFP.

A: SP. Edge velocity was calculated from the displacement, dS (locally normal to the boundary), of each boundary point by comparing consecutive cell contours separated by a time interval, dT, and expressed as dS/dT in μm/min. Color maps were made using Matlab scripts. Space axis is in units of contour points of the cell boundary (see below, same for other edge velocity maps) and time axis is in seconds. Yellow represents protrusion of the cell boundary, and dark blue represents retraction. Red dashed line indicates the time point when polarization is initiated.

B: EFP. An EF of 4 V/cm was applied at the time = 0. Red dashed line indicates the time point when polarization is initiated.

C: Diagrams to show how initial sampling points around cell perimeter are defined upon EF application. Point "0" is always the middle point facing the cathode. Yellow arrow represents protrusion of the cell boundary, and blue arrow represents retraction.

D: Aspect ratios of cells under different EF conditions. Aspect ratio is defined as explained in Figure 1. Data is presented as normalized mean ± SE from combined experiments. **, $p < 0.001$ indicates significant difference compared to no EF control by paired two-sample Student's *t*-test.

$p < 0.001$ indicates significant difference compared to short (6 minutes) EF exposure by paired two-sample Student's *t*-test.

Supplemental Figure 3: EFP in the presence of myosin inhibitor (Blebbistatin).

A: Cell trajectories. Trajectories are plotted for each group of keratocytes undergoing EFP, and subsequently migrating directionally in the presence of mock control (n = 23), or 50 μM myosin inhibitor (BB, n = 19). Data are from sample cells from repeated experiments. Axial units are in pixels. EF strength is 4V/cm in the indicated orientation (arrow points to cathode). Duration iss 30 minutes.

B. Additional edge velocity maps for EFP of the cells in the presence of 50 μM myosin inhibitor. EF strength is 4V/cm. Yellow represents protrusion of the cell boundary, and dark blue represents retraction. The duration of EF application is 900 seconds for the map of the bottom left.

Supplemental Video 1: EF-induced polarization starts from the rear of the cell.

Supplemental Video 2: Stationary cells do not initiate motility in the alternating EF.

Supplemental Video 3: EF-induced polarization in the presence of Blebbistatin is sustained after the EF is turned off.